IEEE Access
Multidisciplinary | Rapid Review | Open Access Journal

Received August 16, 2018, accepted September 27, 2018, date of publication October 1, 2018, date of current version October 25, 2018.

Digital Object Identifier 10.1109/ACCESS.2018.2872953

Partially-Activated Conjugate Beamforming for LoS Massive MIMO Communications

WENDONG LIU[1], (Student Member, IEEE), ZHAOCHENG WANG[1], (Senior Member, IEEE), JIANFEI CAO[2], SHENG CHEN[3,4], (Fellow, IEEE), AND LAJOS HANZO[3], (Fellow, IEEE)

[1]Tsinghua National Laboratory for Information Science and Technology, Department of Electronic Engineering, Tsinghua University, Beijing 100084, China
[2]SONY China Research Laboratory, Beijing 100190, China
[3]School of Electronics and Computer Science, University of Southampton, Southampton SO17 1BJ, U.K.
[4]King Abdulaziz University, Jeddah 21589, Saudi Arabia

Corresponding author: Lajos Hanzo (lh@ecs.soton.ac.uk)

This work was supported in part by the National Natural Science Foundation of China under Grant 61571267, in part by the National High Technology Research and Development Program of China under Grant 2014AA01A704, in part by the Shenzhen Peacock Plan under Grant 1108170036003286, and in part by the Shenzhen Visible Light Communication System Key Laboratory under Grant ZDSYS20140512114229398. The work of L. Hanzo was supported in part by the EPSRC Projects, EP/Noo4558/1 and EP/PO34284/1, in part by the Royal Society's GRCF, and in part by the European Research Council's Advanced Fellow Grant QuantCom.

ABSTRACT A partially activated conjugate beamforming (PACB) is proposed for massive multiple-input multiple-output communications, where the line-of-sight (LoS) channel is dominant. Unlike the conventional conjugate beamforming which activates all the antenna elements to radiate the signals, our PACB activates only a fraction of the antennas by exploiting the spatial structure of LoS channel, and it can mitigate the inter-user interference more effectively, leading to dramatically enhanced downlink spectral efficiency. A low-complexity search algorithm is also introduced to calculate the optimal number of activated antennas. Theoretical analysis and simulation results both confirm that our PACB offers significantly higher downlink spectral efficiency compared to its conventional beamforming counterpart.

INDEX TERMS Partially-activated conjugate beamforming, line-of-sight, massive MIMO, inter-user interference.

I. INTRODUCTION

Massive multiple-input multiple-output (MIMO) offers a promising technology for the next generation wireless communication systems [1]–[4]. Because the asymptotic orthogonality is achievable by employing a large-scale antenna array at the base station (BS), massive MIMO is capable of enhancing both the spectral and energy efficiencies significantly with the aid of linear signal processing [2]. For example, the conjugate beamforming (CB) can be utilized to effectively eliminate the inter-user interference (IUI) between the uncorrelated channels from different users [3]. To ensure the asymptotic orthogonality requires the rich-scattering channel environment, which is generally the case in current wireless communication systems. In this case, the non-line-of-sight (NLoS) component is dominant and the wireless channel can be modeled approximately by a Gaussian distribution with low correlation between different users [1], [2]. To fully explore the potential of spatial diversity and multiplexing gains provided by NLoS channels, advanced beamforming and precoding methodologies have been proposed to enhance the performance of massive MIMO systems [3], [5]–[7].

However, in many new wireless communication applications, the line-of-sight (LoS) channel is dominant. For example, in air-to-air communications, the LoS channel is predominant with litter or no scattering component [8]. Also LoS channels are widely approved in unmanned aerial vehicle (UAV) communications [9], [10]. Firstly, LoS links in low-altitude UAV-ground channels are mostly preferred [10]. In addition, the UAV-UAV and UAV-BS backhaul channels are dominated by LoS components as well, wherein the emerging millimeter-wave (mmWave) MIMO technology is utilized to achieve the high-rate transmissions [9]. In mmWave communications, the pathloss of NLoS channels is relatively high, and LoS signals are mainly considered [11]–[13]. The asymptotic orthogonality is invalid in LoS scenarios due to the higher correlation between various channels from different users [12], which results in higher residual IUI and spectral efficiency (SE) loss. Thus the conventional low-complexity analogue CB suffers from serious

performance degradation in LoS environments, and the hybrid precoding architecture is often preferred [14], [15]. But the joint design of digital and analogue precoders/combiners is a complicated optimization with inherently high complexity [14]–[16]. Moreover, since 5G new radio (NR) requires larger user density and higher SE, serving adjacent users at the same time-frequency resource draws lots of attentions recently [17], [18]. As claimed in [17], non-linear precoding including Tomlinson-Harashima precoding (THP) and vector perturbation (VP) should be investigated to enhance the MU-MIMO performance with adjacent users. However, non-linear precoding methodologies possess high complexity and major channel state information (CSI)-related modifications in practical massive MIMO systems [19]. This motivates us to investigate the efficient low-complexity alternative to the conventional CB, capable of applying to LoS massive MIMO communications, especially with adjacent users.

In this paper, we reveal a fascinating property of LoS scenario, namely, adopting transmit antennas as many as possible for CB may not be a good choice, and using a smaller number of transmit antennas is often capable of mitigating the IUI more effectively. Based on this discovery, a partially-activated conjugate beamforming (PACB) scheme is proposed to exploit the spatial structure of the LoS channel by activating only a fraction of all the antennas, which we prove is capable of realizing a better orthogonality of the channels for different users. Specifically, we prove that by activating a fraction of all the antennas for beamforming, the amplitude of the inner-product between the channel vectors of two different users is much closer to zero, compared to the case of adopting all the antennas for beamforming. Thus, the IUI is reduced considerably and the signal-to-interference plus noise ratio (SINR) is improved significantly. The optimal number of activated antennas can be determined by maximizing the system's capacity or SINR using an exhaustive search, which has the complexity on the order of $\mathsf{O}(M_{\mathrm{t}})$, where M_{t} is the number of available antennas. A even lower complexity search algorithm is also derived to calculate the number of the activated antennas by maximizing the system's signal-to-interference ratio (SIR). Both theoretical analysis and simulation study confirm that the system's SE achieved by this low-complexity search is indistinguishable from the optimal performance attained by the exhaustive search under high signal-to-noise ratio (SNR) conditions. Theoretical analysis and simulation results also validate the superior SE of our PACB scheme over the conventional CB.

It must be pointed out that our PACB for LoS massive MIMO is completely different from the subset antenna selection for MIMO under a rich-scattering environment. In the latter case, to reduce the required radio-frequency (RF) chains to N, where $N < M_{\mathrm{t}}$, subset antenna selection is carried out to select a subset of N antennas from the full set of M_{t} antennas [20]. The optimal subset antenna selection has the complexity on the order of $\mathsf{O}\left(\binom{M_{\mathrm{t}}}{N}\right)$, which is impossible to do even for a modest M_{t}. Critically, in rich-scattering environments, the performance of the optimal N-antenna system is always worst than that of the full M_{t}-antenna system. By contrast, in LoS environments, our PACB with a complexity much lower than $\mathsf{O}(M_{\mathrm{t}})$ simply activates the first N_{o} antennas, and its performance is better than that of employing all the M_{t} antennas. The recent works [21], [22] randomly select N antennas from the full set of M_{t} antennas to enhance mmWave communication security, which is obviously different from our PACB.

II. SYSTEM MODEL

A. TRANSMISSION AND CHANNEL MODEL

Consider a mmWave BS employs a uniformly-spaced linear array (ULA) having M_{t} transmit antennas to support I mobile users using the same time/frequency resource block. To highlight the underlying physics and without loss of generality, we restrict our analysis mainly to the case of $I = 2$. However, latter we will extend our PACB to the generic case of $I > 2$.

Each user is equipped with a ULA of M_{r} antennas. Denote $\boldsymbol{H}_i \in \mathbb{C}^{M_{\mathrm{r}} \times M_{\mathrm{t}}}$ as the downlink channel matrix between the BS and the ith user, and let x_i be the transmitted symbol to user i, where $i = 1, 2$. The BS performs the transmit beamforming on x_i with the beamforming vector $\boldsymbol{f}_i \in \mathbb{C}^{M_{\mathrm{t}} \times 1}$. The total power constraint with $E\{\boldsymbol{x}\boldsymbol{x}^{\mathrm{H}}\} = \frac{1}{2}\boldsymbol{I}_2$ and $||\boldsymbol{F}||_{\mathrm{F}}^2 = 2$ are utilized [14], wherein $E\{\cdot\}$ and $||\cdot||_{\mathrm{F}}$ represent the expectation and Frobenius norm, respectively. $\boldsymbol{x} = [x_1, x_2]^{\mathrm{T}}$ is the transmitted symbol vector and $\boldsymbol{F} = [\boldsymbol{f}_1, \boldsymbol{f}_2]$ denotes the beamforming matrix at the BS. User i carries out the combining operation on the signals received at its M_{r} antennas with the combining vector $\boldsymbol{w}_i \in \mathbb{C}^{M_{\mathrm{r}} \times 1}$. Thus, the received symbol y_i by the ith user can be expressed as

$$y_i = \boldsymbol{w}_i^{\mathrm{T}} \boldsymbol{H}_i \boldsymbol{f}_i x_i + \boldsymbol{w}_i^{\mathrm{T}} \boldsymbol{H}_i \boldsymbol{f}_{i'} x_{i'} + n_i, \quad i, i' = 1, 2, \ i' \neq i, \quad (1)$$

where $(\cdot)^{\mathrm{T}}$ denotes the transpose operator, and n_i is the additive white Gaussian noise (AWGN) with power σ_n^2. The term $\boldsymbol{w}_i \boldsymbol{H}_i \boldsymbol{f}_{i'} x_{i'}$ represents the IUI.

The channel model for $\boldsymbol{H}_i$ is given by [14]

$$\boldsymbol{H}_i = \gamma \sum_{p=0}^{P} \alpha_p \boldsymbol{H}_{i,p} = \gamma \sum_{p=0}^{P} \alpha_p \boldsymbol{h}_{\mathrm{r}}(\theta_{i,p}) \boldsymbol{h}_{\mathrm{t}}^{\mathrm{T}}(\varphi_{i,p}), \quad (2)$$

in which $\boldsymbol{H}_{i,0}$ and $\boldsymbol{H}_{i,p}$, $1 \leq p \leq P$ represent the LoS and NLoS channel components, respectively, wherein P is the total number of NLoS sub-paths. α_p denotes the complex gain associated with the p-th sub-path. γ is the channel normalization factor to ensure $E\{||\boldsymbol{H}_i||_{\mathrm{F}}^2\} = M_{\mathrm{t}} M_{\mathrm{r}}$. Furthermore, with antenna spacing $D = \lambda/2$, where λ is the carrier wavelength, the channel response vectors $\boldsymbol{h}_{\mathrm{r}}(\theta_{i,p})$ and $\boldsymbol{h}_{\mathrm{t}}(\varphi_{i,p})$ for the p-th sub-path with the angle-of-arrival (AoA) $\theta_{i,p}$ at the user and the angle-of-departure (AoD) $\varphi_{i,p}$ at the BS can be written as

$$\boldsymbol{h}_{\mathrm{r}}(\theta_{i,p}) = \left[1 \ e^{-\mathrm{j}\pi \cos\theta_{i,p}} \cdots e^{-\mathrm{j}\pi(M_{\mathrm{r}}-1)\cos\theta_{i,p}}\right]^{\mathrm{T}}, \quad (3)$$

$$\boldsymbol{h}_{\mathrm{t}}(\varphi_{i,p}) = \left[1 \ e^{-\mathrm{j}\pi \cos\varphi_{i,p}} \cdots e^{-\mathrm{j}\pi(M_{\mathrm{t}}-1)\cos\varphi_{i,p}}\right]^{\mathrm{T}}, \quad (4)$$

In typical mmWave scenario, LoS channel is dominant with fewer number of NLoS sub-paths P [23]. Meanwhile, due to the relatively larger path-loss of NLoS sub-paths, $|\alpha_0|$ is 5dB to 10dB stronger than $|\alpha_p|$, $1 \le p \le P$ [23].

B. PROBLEM FORMULATION

Here, denoting $\boldsymbol{h}_i = \boldsymbol{h}_{\rm t}(\varphi_{i,0})$ and adopting the conjugate beamforming/combining, we have $\boldsymbol{f}_i = \frac{1}{\sqrt{M_{\rm t}}}\boldsymbol{h}_i^*$ and $\boldsymbol{w}_i = \frac{1}{\sqrt{M_{\rm r}}}\boldsymbol{h}_r^*(\theta_i)$, where $(\cdot)^*$ denotes the conjugate operator. Considering the symmetry of the two users, the achievable average downlink SE C_2 is formulated as

$$C_2 = \log_2\left(1 + \frac{M_{\rm t}M_{\rm r}}{M_{\rm r}|\boldsymbol{h}_1^{\rm T}\boldsymbol{f}_2|^2 + \sigma_n^2}\right). \tag{5}$$

Note that the asymptotic orthogonality of conventional massive MIMO is invalid here because of the high correlation between the LoS channels $\boldsymbol{h}_1$ and $\boldsymbol{h}_2$, which produces severe IUI, reducing the downlink SE considerably. Furthermore, the following fact stated in Lemma 1 does not seem to be widely recognized.

Lemma 1: For strong LoS channels, employing as many as possible transmit antennas is generally a bad choice.

Proof: By denoting $\varepsilon = |\cos\varphi_1 - \cos\varphi_2|$, the magnitude of the IUI $|\boldsymbol{h}_1^{\rm T}\boldsymbol{f}_2|$ is given as

$$\begin{aligned}|\boldsymbol{h}_1^{\rm T}\boldsymbol{f}_2| &= \frac{1}{\sqrt{M_{\rm t}}}\left|\sum_{m=0}^{M_{\rm t}} e^{{\rm j}\pi m\varepsilon}\right| = \frac{1}{\sqrt{M_{\rm t}}}\left|\frac{1-e^{{\rm j}\pi M_{\rm t}\varepsilon}}{1-e^{{\rm j}\pi\varepsilon}}\right| \\ &= \frac{1}{\sqrt{M_{\rm t}}}\left|\frac{\sin\frac{\pi M_{\rm t}\varepsilon}{2}}{\sin\frac{\pi\varepsilon}{2}}\right| \triangleq \frac{1}{\sqrt{M_{\rm t}}}A(M_{\rm t},\varepsilon) \\ &= \frac{\sqrt{M_{\rm t}}}{\left|\mathrm{sinc}\frac{\pi\varepsilon}{2}\right|}\left|\mathrm{sinc}\frac{\pi M_{\rm t}\varepsilon}{2}\right| \to \sqrt{M_{\rm t}}, \quad \varepsilon \to 0. \end{aligned} \tag{6}$$

Thus, employing more transmit antennas may lead to higher interference, particularly when the two users are adjacent. ■

The correlations of the two users' channel vectors, $\boldsymbol{h}_1$ and $\boldsymbol{h}_2$, as the function of $M_{\rm t}$ under the LoS and NLoS conditions, respectively, are compared in Fig. 1, where the two users' AoDs are $\varphi_1 = 90°$ and $\varphi_2 = 85°$, respectively. In the NLoS MIMO with complex Gaussian channel, the correlation between two channel vectors is reduced monotonously with the increase of $M_{\rm t}$, and the asymptotic orthogonality is only achieved as $M_{\rm t} \to \infty$. Furthermore, the achievable performance of employing $N = 206$ transmit antennas is worst than that achieved by employing all the $M_{\rm t} = 256$ antennas. By contrast, in the LoS channel condition, the correlation exhibits oscillating and damping as $M_{\rm t}$ increases, and it also becomes zero with specific final $M_{\rm t}$ values, e.g., red points. Consequently, employing $N = 206$ transmit antennas outperforms the case of employing all the $M_{\rm t} = 256$ antennas.

Remark 1: The actual amount of IUI does not depend on the number of transmit antennas $M_{\rm t}$ alone. Rather, it is determined by the product of $M_{\rm t}$ and ε, the latter specifying the spatial structure of LoS channels. The sinc function is quasi-periodic with many zero cross points. It can readily be seen that if $\frac{\pi M_{\rm t}\varepsilon}{2}$ happens to be such a zero cross point, the IUI vanishes. This motivates our PACB. Specifically, rather than activating all the $M_{\rm t}$ transmit antennas as in the conventional CB, we only activate a fraction of the antennas, say N antennas, where obviously $2 \le N \le M_{\rm t}$. By choosing an appropriate N, we can let $\frac{\pi N\varepsilon}{2}$ to be at or near a zero cross point of the sinc function, and this will dramatically reduce the IUI.

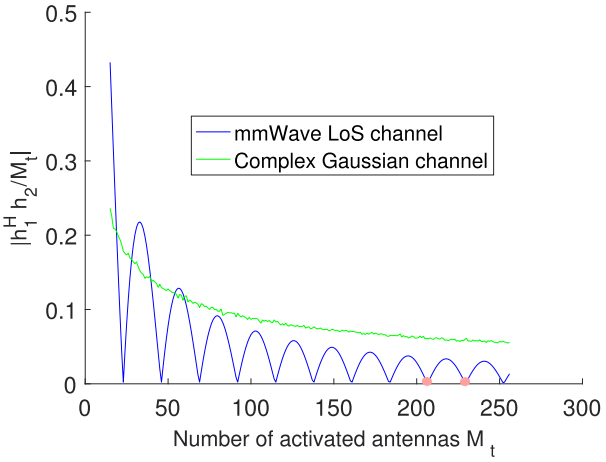

FIGURE 1. Comparison of the correlations for the mmWave LoS and complex Gaussian NLoS channels.

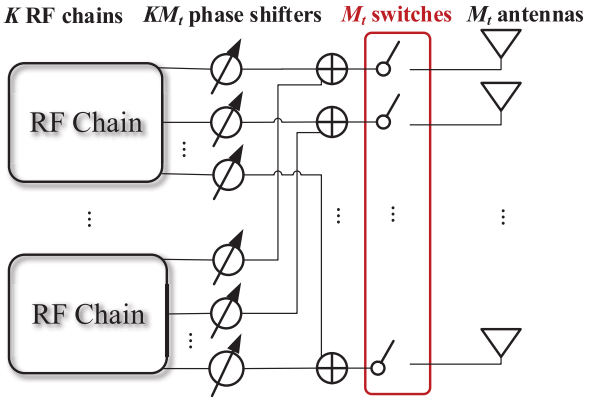

FIGURE 2. Analogue beamforming structure: for conventional CB, all the $M_{\rm t}$ switches are closed, while for PACB, only the first N switches are closed.

III. PROPOSED SCHEME

A. PARTIALLY-ACTIVATED CONJUGATE BEAMFORMING

The transmitter structures of the conventional CB and the proposed PACB are both depicted in Fig. 2. Assuming K RF chains, $KM_{\rm t}$ phase shifters are utilized to perform the analogue beamforming based on the full-connection structure [9]. For the conventional CB, all the $M_{\rm t}$ transmit antennas are activated, corresponding to close all the $M_{\rm t}$ switches in Fig. 2. By contrast, the PACB only activates the first N antennas, which corresponds to close the first N switches

in Fig. 2. Hence, the PACB vector $\boldsymbol{f}_i$ is expressed as

$$\boldsymbol{f}_i = \frac{1}{\sqrt{N}}\left[1\ e^{\mathrm{j}\pi\cos\varphi_i}\cdots e^{\mathrm{j}\pi(N-1)\cos\varphi_i}\ \mathbf{0}^{\mathrm{T}}_{(M_\mathrm{t}-N)\times 1}\right]^{\mathrm{T}}, \quad (7)$$

where the $(M_\mathrm{t}-N)\times 1$ zero vector $\mathbf{0}_{(M_\mathrm{t}-N)\times 1}$ indicates that the corresponding antenna elements $N \le m \le M_\mathrm{t}-1$ are turned off. We first assume the two-user case. Substituting $\boldsymbol{f}_i$ of (7) for $i=1,2$ into (5) yields

$$C_2(N) = \log_2\left(1+\frac{1}{\frac{1}{N^2}A(N,\varepsilon)^2+\frac{1}{NM_\mathrm{r}}\sigma_n^2}\right). \quad (8)$$

The optimal number of activated antennas, N_o, which maximizes the capacity $C_2(N)$ of (8), is obtained as follows

$$N_\mathrm{o} = \arg\max_{2\le N\le M_\mathrm{t}} C_2(N). \quad (9)$$

The exhaustive search with the complexity on the order of $\mathbf{O}(M_\mathrm{t})$ can be employed to calculate N_o.

Remark 2: Unlike the average SE of the NLoS massive MIMO, which is monotonously increasing with M_t, the average SE of the LoS massive MIMO exhibits the oscillating and increasing characteristics as M_t increases, owing to its IUI characteristics shown in Fig. 1. Fig. 3 compares the average downlink SEs of the mmWave LoS and complex Gaussian NLoS channels, where the two users' AoDs are $\varphi_1 = 90°$ and $\varphi_2 = 85°$, respectively, while the AWGN power is $\sigma_n^2 = 1$. Observe that $N_\mathrm{o} = 252$, which is smaller than $M_\mathrm{t} = 256$. In fact, even by only activating first $N = 22$ antennas, we have $C_2(22) > C_2(256)$, which is remarkable.

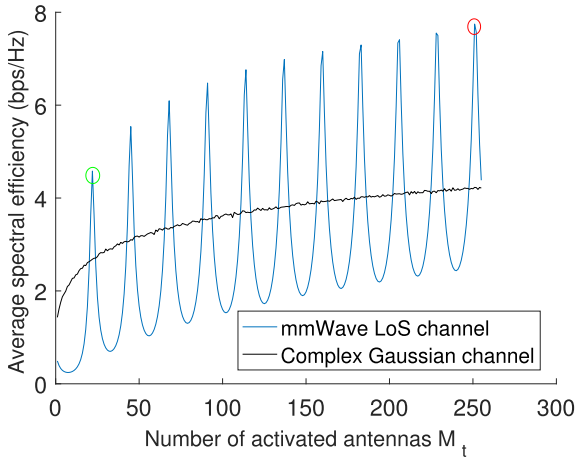

FIGURE 3. Comparison of the average downlink capacities for the mmWave LoS and complex Gaussian NLoS channels.

It is highly desired to derive an even lower complexity search algorithm, particularly, if the solution found by such a low-complexity algorithm is at least a near optimal solution. Let us consider the two special cases of (9).

1) In extremely high noisy scenarios, where the noise is dominant and the interference is small by comparison, the SINR can be approximated by the SNR of $\frac{NM_\mathrm{r}}{\sigma_n^2}$, which indicates that the optimal solution to the optimization problem (9) is approximately $N_\mathrm{o} = M_\mathrm{t}$, the fully activated beamforming.

2) In massive MIMO, the IUI is generally dominant and the effect of the noise is negligible by comparison. Hence, the SINR can be approximated by the SIR. This indicates that a suboptimal solution N_s to the optimization problem (9) can be obtained as the solution of the following optimization

$$N_\mathrm{s} = \arg\max_{2\le N\le M_\mathrm{t}} \frac{N}{A(N,\varepsilon)} = \arg\max_{2\le N\le M_\mathrm{t}} \left|\frac{N\sin\frac{\pi\varepsilon}{2}}{\sin\frac{\pi N\varepsilon}{2}}\right|. \quad (10)$$

The optimization (10) is equivalent to the optimization (9) by neglecting the noise power in the capacity formula (8).

B. LOW-COMPLEXITY SEARCHING ALGORITHM

Since the denominator $\sin\frac{\pi N\varepsilon}{2}$ in the optimization (10) is quasi-periodic, we can select the value of N_s to let $\sin\frac{\pi N_\mathrm{s}\varepsilon}{2} \to 0$ in order to reduce the IUI dramatically. Ignoring the effect of the linear factor N, (10) can be further expressed as

$$N_\mathrm{s} = \arg\min_{2\le N\le M_\mathrm{t}} \left|\sin\frac{\pi N\varepsilon}{2}\right|. \quad (11)$$

The solution to the optimization (11) is to let $\frac{N\varepsilon}{2}$ be the closest to an integer, specifically,

$$N_\mathrm{s} = \arg\min_{2\le N\le M_\mathrm{t}} \left|\frac{N\varepsilon}{2}-\left\lfloor\frac{N\varepsilon}{2}\right\rceil\right|, \quad (12)$$

where the operator $\lfloor\cdot\rceil$ denotes the proximal integer. Since ε is small and in the limit case $\varepsilon\to 0$, we can express $\frac{2}{\varepsilon} = T+t$, in which t denotes the fractional part and

$$T = \left\lfloor\frac{2}{\varepsilon}\right\rfloor \ge 1 \quad (13)$$

is the integer part, where $\lfloor\cdot\rfloor$ stands for the integer floor operator. Further denote the residual function

$$q(N) = \left|\frac{N\varepsilon}{2}-\left\lfloor\frac{N\varepsilon}{2}\right\rceil\right|. \quad (14)$$

Clearly, we can decompose N into

$$N = nT+l, \quad (15)$$

where n is the index of the periodicity with period T and $0\le l\le T-1$ is the remainder. Then $q(N)$ can be simplified as

$$\begin{aligned} q(N) = q(nT+l) &= \left|\frac{nT\varepsilon}{2}+\frac{l\varepsilon}{2}-\left\lfloor\frac{nT\varepsilon}{2}+\frac{l\varepsilon}{2}\right\rceil\right| \\ &= \left|n\left(\frac{2}{\varepsilon}-t\right)\frac{\varepsilon}{2}+\frac{l\varepsilon}{2}-\left\lfloor n\left(\frac{2}{\varepsilon}-t\right)\frac{\varepsilon}{2}+\frac{l\varepsilon}{2}\right\rceil\right| \\ &= \left|(l-nt)\frac{\varepsilon}{2}-\left\lfloor(l-nt)\frac{\varepsilon}{2}\right\rceil\right| = \left|\frac{l-nt}{T+t}-\left\lfloor\frac{l-nt}{T+t}\right\rceil\right|. \end{aligned} \quad (16)$$

Similarly, we can decompose $\frac{nt}{T+t}$ into the two parts as

$$\begin{aligned} \frac{nt}{T+t} &= \left\lfloor\frac{nt}{T+t}\right\rfloor+\left(\frac{nt}{T+t}-\left\lfloor\frac{nt}{T+t}\right\rfloor\right) \\ &\triangleq G(n)+g(n), \end{aligned} \quad (17)$$

with $G(n)$ and $g(n)$ denoting the integer part and fractional part, respectively. Substituting (17) to (16) yields

$$q(N) = \left| \frac{l}{T+t} - g(n) - \left\lfloor \frac{l}{T+t} - g(n) \right\rceil \right|. \quad (18)$$

Considering $0 \le \frac{l}{T+t} < 1$ and $0 \le g(n) < 1$, we have

$$b(l,n) = \frac{l}{T+t} - g(n) \in (-1,\ 1). \quad (19)$$

Therefore, (18) can be rewritten as

$$q(N) = \begin{cases} 1 + b(l,n), & b(l,n) \in \left(-1,\ -\frac{1}{2}\right), \\ -b(l,n), & b(l,n) \in \left[-\frac{1}{2},\ 0\right), \\ b(l,n), & b(l,n) \in \left[0,\ \frac{1}{2}\right), \\ 1 - b(l,n), & b(l,n) \in \left[\frac{1}{2},\ 1\right). \end{cases} \quad (20)$$

Given the index of periodicity n, we have $0 \le l \le T-1$, and $b(l,n)$ takes the value from the finite set of T values, namely,

$$b(l,n) \in \left\{ -g(n),\ \frac{1}{T+t} - g(n),\ \cdots,\ \frac{T-1}{T+t} - g(n) \right\}, \quad (21)$$

where $-g(n) \le 0$ and $\frac{T-1}{T+t} - g(n) < 1$. Further observe from (20) that $q(N)$ attains its local-minimum when $b(l,n) \to -1$, 0 or 1. Therefore, the possible candidates of l to achieve the minimum of $q(N)$ can be obtained only on the boundaries with $l = 0, T-1, l_n^-$ or l_n^+, where $l_n^+ = l_n^- + 1$, satisfying

$$\frac{l_n^-}{T+t} - g(n) < 0 < \frac{l_n^+}{T+t} - g(n). \quad (22)$$

First, consider the potential candidates l_n^- and l_n^+ by defining

$$q(N_n) = \min\left\{ q(nT + l_n^-),\ q(nT + l_n^+) \right\}. \quad (23)$$

Since the length of the interval $\left[\frac{l_n^-}{T+t} - g(n),\ \frac{l_n^+}{T+t} - g(n) \right]$ is $\frac{1}{T+t}$, $q(N_n)$ is upper bounded by $\frac{1}{2(T+t)}$, that is,

$$q(N_n) \le \frac{1}{2(T+t)} = \frac{\varepsilon}{4}. \quad (24)$$

Next, consider the other two potential candidates $l = 0$ and T. At $l = 0$ or T, $q(N)$ depends on the fractional part $g(n)$, which follows the uniform distribution in $[0,\ 1)$ and, therefore, has the average value of 0.5. Thus, at $l = 0$ or T the value of $q(N)$ is typically much larger than $\frac{\varepsilon}{4}$. Consequently, we can rule out $l = 0$ and T. Hence, given n, the single local-minimum solution is at $l = l_n^-$ or l_n^+, specified by (23).

Once we have l_n^- and l_n^+, the next pair of indexes l_{n+1}^- and l_{n+1}^+ can be obtained by the forward recursion. Specifically, based on (17), $g(n+1)$ is calculated by

$$\begin{aligned} g(n+1) &= g(n) + \frac{t}{T+t} - \left\lfloor g(n) + \frac{t}{T+t} \right\rfloor \\ &= \begin{cases} g(n) + \dfrac{t}{T+t}, & G(n+1) = G(n), \\ g(n) + \dfrac{t}{T+t} - 1, & G(n+1) = G(n) + 1. \end{cases} \end{aligned} \quad (25)$$

As for the first condition with $G(n+1) = G(n)$, we have

$$\begin{aligned} \frac{l_{n+1}^-}{T+t} - g(n+1) < 0 < \frac{l_{n+1}^+}{T+t} - g(n+1) \\ \Leftrightarrow \frac{l_{n+1}^- - 1}{T+t} - g(n) < 0 < \frac{l_{n+1}^+ - 1}{T+t} - g(n) \\ \Leftrightarrow l_{n+1}^- - 1 \le l_n^- \quad \text{and } l_{n+1}^+ - 1 \ge l_n^+. \end{aligned} \quad (26)$$

Considering $l_n^+ = l_n^- + 1$, we obtain

$$l_{n+1}^- = l_n^+ \text{ and } l_{n+1}^+ = l_n^+ + 1. \quad (27)$$

Under the second condition with $G(n+1) = G(n)+1$, similar to (26), l_{n+1}^- satisfies

$$l_n^+ + (T+t) \le l_{n+1}^- \le l_n^- + (T+t) + 1. \quad (28)$$

Restricting $0 \le l \le T-1$, the forward recursions in (27) and (28) can be collectively formulated as

$$l_{n+1}^- = l_n^+ \text{ and } l_{n+1}^+ = \left(l_n^+ + 1\right) \mod T, \quad (29)$$

where mod stands for the modulo operator.

Starting from the initial index $n = 1$ with $l_1^- = 0$, therefore, we can obtain all the candidate indexes by the forward recursion (29) and consequently derive the candidate set

$$\mathbb{S} = \left\{ N_n | N_n \text{ given by (23)} \right\}. \quad (30)$$

It is obvious from the above derivation that the optimization (10) is identical to the following optimization

$$N_s = \arg\max_{N \in \mathbb{S}} \frac{N}{A(N,\varepsilon)}. \quad (31)$$

The complexity of solving the optimization (31) is on the order of $\mathsf{O}(|\mathbb{S}|)$, where $|\mathbb{S}|$ is the cardinal of $\mathbb{S}$. For small ε, T is large and we have $|\mathbb{S}| \approx \frac{M_t}{T} \ll M_t$. Therefore, our low-complexity search imposes much lower complexity than the exhaustive search to find a near optimal solution N_s. For example, when $\varphi_1 = 90°$ and $\varphi_2 = 85°$, we have $\varepsilon = 0.0872$ and $T = 22$, which means that the complexity is at least one order of magnitude lower than the exhaustive search.

C. PERFORMANCE ANALYSIS

As pointed out previously, with all the M_t transmit antennas activated, the magnitude of the IUI $\frac{1}{\sqrt{M_t}} A(M_t, \varepsilon)$ is typically large, especially when ε is small, i.e., the two users are close. The PACB, by activating only the N_s transmit antennas, reduces the IUI $\frac{1}{\sqrt{N_s}} A(N_s, \varepsilon)$ dramatically. An upper-bound of $\frac{1}{\sqrt{N_s}} A(N_s, \varepsilon)$ is derived as follows. Noting (24), we have

$$\begin{aligned} \left| \sin \frac{\pi N_s \varepsilon}{2} \right| &= \left| \sin \pi \left(\left\lfloor \frac{N_s \varepsilon}{2} \right\rceil \pm q(N_s) \right) \right| \\ &= \sin \pi q(N_s) \le \sin \frac{\pi \varepsilon}{4}. \end{aligned} \quad (32)$$

Therefore, we have

$$\begin{aligned} \frac{1}{\sqrt{N_s}} A(N_s, \varepsilon) &= \frac{1}{\sqrt{N_s}} \left| \frac{\sin \frac{\pi N_s \varepsilon}{2}}{\sin \frac{\pi \varepsilon}{2}} \right| \le \frac{1}{\sqrt{N_s}} \left| \frac{\sin \frac{\pi \varepsilon}{4}}{\sin \frac{\pi \varepsilon}{2}} \right| \\ &\approx \frac{1}{2\sqrt{N_s}}, \end{aligned} \quad (33)$$

where the approximation is due to $\sin\varepsilon \to \varepsilon$ with $\varepsilon \to 0$. It can readily be seen that typically

$$\frac{1}{\sqrt{N_s}}A(N_s,\varepsilon) \ll \frac{1}{\sqrt{M_t}}A(M_t,\varepsilon). \tag{34}$$

Denote the downlink SEs achieved by M_t, N_s and N_o as $C_f = C_2(M_t)$, $C_s = C_2(N_s)$ and $C_o = C_2(N_o)$, respectively. Although the noise power $\frac{1}{N_s M_r}\sigma_n^2$ in the PACB is slightly larger than the noise power $\frac{1}{M_t M_r}\sigma_n^2$ in the fully activated case, its IUI power $\frac{1}{N_s^2}A^2(N_s,\varepsilon)$ is significantly lower than $\frac{1}{M_t^2}A^2(M_t,\varepsilon)$. Since the interference power is much larger than the noise power, we can conclude that $C_s \gg C_f$, except in the high noise case. It can also easily be seen that $C_s \le C_o$, and the equality holds when $\sigma_n^2 \to 0$. Since the system is interference limited, C_s is very close to C_o, that is, $C_s \approx C_o$.

Furthermore, some insights about the effect of ε on N_s are provided. Based on the forward recursion in (29), the candidate N_s occurs quasi-periodically with period T. Moreover, to guarantee sufficient power of received signal, the largest N_s candidate in $\mathbb{S}$ is preferred. Therefore, although we cannot obtain the exact value of N_s explicitly, we have the following constrain on N_s,

$$N_s \ge M_t - T = M_t - \left\lfloor \frac{2}{\varepsilon} \right\rfloor, \tag{35}$$

which indicates that N_s is closer to M_t with relatively larger ε. For example, equipping $M_t = 256$ antennas at the BS and assuming $\varphi_1 = 90°$, $\varphi_2 = 85°$, we have $T = 22$ and $N_s = 252$. As comparison, if $\varphi_1 = 90°$, $\varphi_2 = 88°$, we obtain $T = 57$ and $N_s = 228$.

Next, the SE averaged over the distribution of AoDs is presented. Combining (8) with (33) and ignoring the effect of noise, we have the lower-bound as

$$C_2(N_s) \ge \log_2\left(1 + 4N_s^2\cos^2\frac{\pi\varepsilon}{4}\right), \tag{36}$$

Due to the analytical difficulty of directly calculating the expectation of $C_2(N_s)$ over different φ_1, φ_2, we turn to focus on the average SE over various ε to address this point. Specifically, ε is assumed uniformly distributed in $(\varepsilon_{\min}, \varepsilon_{\max})$. Hence, $E\{C_2(N_s)\}$ can be expressed as

$$\begin{aligned} E\{C_2(N_s)\} &= \frac{1}{\varepsilon_{\max}-\varepsilon_{\min}}\int_{\varepsilon_{\min}}^{\varepsilon_{\max}} \log_2\left(1 + 4N_s^2\cos^2\frac{\pi\varepsilon}{4}\right)d\varepsilon \\ &\ge \frac{2}{\varepsilon_{\max}-\varepsilon_{\min}}\int_{\varepsilon_{\min}}^{\varepsilon_{\max}} \left(\log_2 2N_s + \log_2\cos\frac{\pi\varepsilon}{4}\right)d\varepsilon \\ &\overset{(a)}{\ge} 2\log_2 2(M_t - T_{\min}) \\ &\quad + \frac{2}{\varepsilon_{\max}-\varepsilon_{\min}}\int_{\varepsilon_{\min}}^{\varepsilon_{\max}} \log_2\cos\frac{\pi\varepsilon}{4}d\varepsilon \\ &\overset{(b)}{\ge} 2\log_2 2(M_t - T_{\min}) - \frac{4}{\varepsilon_{\max}-\varepsilon_{\min}} \end{aligned} \tag{37}$$

s wherein (a) is given from (35) by denoting $T_{\min} = \left\lfloor \frac{2}{\varepsilon_{\min}} \right\rfloor$ as the periodic of N_s with $\varepsilon_{\min}$. (b) is valid because of $\varepsilon \in (\varepsilon_{\min}, \varepsilon_{\max}) \subset (0, 2)$ and the definite integral $\int_0^{\pi/2} \ln\cos x dx = -\frac{\pi}{2}\ln 2$. Observed from (37), we find that the proposed PACB is capable of providing sufficient spatial multiplexing gain offered by large-scale antenna array at the BS. This result proves that PACB is still adequately valid when considering the effect of AoD distribution, not just for the case of adjacent users discussed above.

D. ANALYSES FOR AOD ESTIMATION ERROR

Denoting $\varepsilon' = \varepsilon + \Delta\varepsilon$, wherein $\Delta\varepsilon$ represents the AoD gap error caused by AoD estimation error, BS calculates the corresponding number of activated antennas N_s' and average SE $C_2(N_s')$. Generally, $\Delta\varepsilon/\varepsilon \ll 1$ is assumed, which is reasonable by adopting large-scale antenna array at the BS along with advanced AoD estimation methodologies [24]. Similar to (32), we have

$$\begin{aligned} \left|\sin\frac{\pi N_s'\varepsilon}{2}\right| &= \left|\sin\pi\left(q(N_s') \pm \left\lfloor\frac{N_s'\varepsilon'}{2}\right\rceil - \frac{N_s'\Delta\varepsilon}{2}\right)\right| \\ &= \left|\sin\pi\left(q(N_s') - \frac{N_s'\Delta\varepsilon}{2}\right)\right| \\ &\le \left|\sin\pi q(N_s')\right|\left|\cos\frac{\pi N_s'\Delta\varepsilon}{2}\right| \\ &\quad + \left|\cos\pi q(N_s')\right|\left|\sin\frac{\pi N_s'\Delta\varepsilon}{2}\right| \\ &\le \frac{\pi\varepsilon'}{4} + \left|\frac{\pi N_s'\Delta\varepsilon}{2}\right|. \end{aligned} \tag{38}$$

Therefore, we have

$$\begin{aligned} \frac{1}{\sqrt{N_s'}}A(N_s',\varepsilon) &\le \frac{1}{\sqrt{N_s'}}\left|\frac{\frac{\pi\varepsilon'}{4} + \left|\frac{\pi N_s'\Delta\varepsilon}{2}\right|}{\sin\frac{\pi\varepsilon}{2}}\right| \\ &\approx \frac{1}{\sqrt{N_s'}}\left(0.5 + (0.5 + N_s')\frac{\Delta\varepsilon}{\varepsilon}\right), \end{aligned} \tag{39}$$

which is readily smaller than $\frac{1}{\sqrt{M_t}}A(M_t,\varepsilon)$ with conventional CB and indicates lower IUI between two users.

Remark 3: Readily, the proposed PACB still outperforms conventional CB with moderately small AoD estimation error in general cases. Moreover, a pre-detection can be added to avoid the performance degradation with large AoD estimation error and hence improves the robustness of the proposed PACB methodology. Specifically, if $C_2(N_s') > C_f$, BS activates N_s' antennas for beamforming, otherwise conventional CB is performed by activating all M_t antennas.

E. PACB FOR $I > 2$

The SINR of the ith user, where $1 \le i \le I$, is

$$\mathrm{SINR}_i(N) = \frac{|\boldsymbol{h}_i^{\mathrm{T}}\boldsymbol{f}_i|^2}{\sum_{l=1,l\ne i}^{I}|\boldsymbol{h}_i^{\mathrm{T}}\boldsymbol{f}_l|^2 + \sigma_n^2} = \frac{N}{\sum_{l=1,l\ne i}^{I}\frac{A(N,\varepsilon_{l,i})^2}{N} + \sigma_n^2}, \ s \tag{40}$$

where $\varepsilon_{l,i} = |\cos\varphi_l - \cos\varphi_i|$. Thus the average downlink SE can be expressed as

$$C_I(N) = \frac{1}{I}\sum_{i=1}^{I}\log_2\left(1 + \mathrm{SINR}_i(N)\right). \tag{41}$$

The optimal number of activated antennas, $N_{\rm o}$, is given by

$$N_{\rm o} = \arg \max_{2 \le N \le M_{\rm t}} C_I(N). \tag{42}$$

The exhaustive search to find $N_{\rm o}$ has the complexity $\mathbf{O}(M_{\rm t})$.

Similar to (30), for each pair of users, we can derive the candidate set $\mathbb{S}_{i,l} = \{N_{i,l,n}\}$, where $1 \le i < l \le I$. Then the intersection set of all the $\mathbb{S}_{i,l}$ is formed

$$\mathbb{S} = \bigcap_{1 \le i < l \le I} \mathbb{S}_{i,l}. \tag{43}$$

To avoid $\mathbb{S} = \emptyset$, we perform a post-process on all the $\mathbb{S}_{i,l}$ as

$$\mathbb{S}_{i,l} = \left\{ N \middle| |N - N_{i,l,n}| \le \mu_{i,l} \right\}, \tag{44}$$

where $\mu_{i,l}$ is the offset for $\mathbb{S}_{i,l}$. By also including N values that are close to $N_{i,l,n}$, the sets $\mathbb{S}_{i,l}$ are enlarged to ensure that $\mathbb{S}$ could not be an empty set. A near optimal solution to $N_{\rm o}$ can then be obtained by solving the optimization problem

$$N_{\rm s} = \arg \max_{N \in \mathbb{S}} \bar{C}_I(N), \tag{45}$$

where $\bar{C}_I(N)$ is the SE by ignoring the noise term in (40).

IV. SIMULATION RESULTS

We consider four two-user cases and one four-user case.

A. CASE ONE (TWO-USER)

The BS is equipped with $M_{\rm t} = 128$ transmit antennas, while each of the two users employs $M_{\rm r} = 16$ receive antennas. The system's normalized SNR is defined as SNR $= 1/\sigma_n^2$. The two AoDs φ_1 and φ_2 are generated to depict the scenario of two adjacent users. Specifically, $\varphi_2 = \varphi_1 + \delta$, where the difference in the AoDs δ, representing the closeness of the two users, is uniformly distributed in $\left(0,\ 5^\circ\right)$.

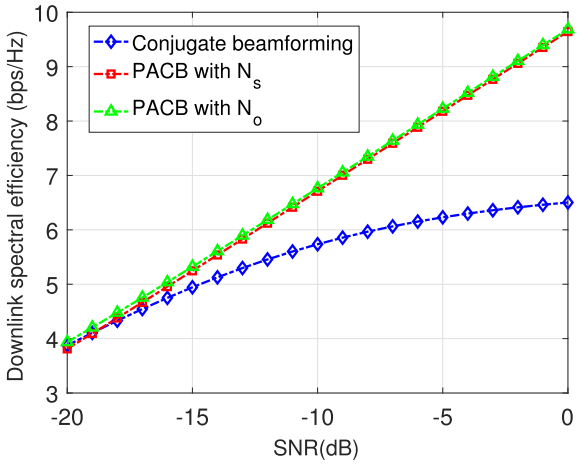

FIGURE 4. Case one (two-user): comparison of average SE for different SNRs.

Fig. 4 compares the downlink SEs achieved by the conventional CB and the PACB as the functions of SNR. Except for the extremely high noise situation, where the optimal solution is to activate all the antennas, i.e., $N_{\rm o} = M_{\rm t}$, we observe the significantly SE gain of the PACB over the conventional CB that activates all the $M_{\rm t}$ antennas. The higher the system's SNR is, the higher this gain becomes. With SNR $=$ 0 dB, for example, $C_{\rm s}$ is 30% larger than $C_{\rm f}$. From Fig. 4, we also observe that except for the extremely high noise situation, $C_{\rm s}$ is indistinguishable from $C_{\rm o}$. This confirms the performance analysis presented in Section III-C, specifically, $C_{\rm s} \approx C_{\rm o}$.

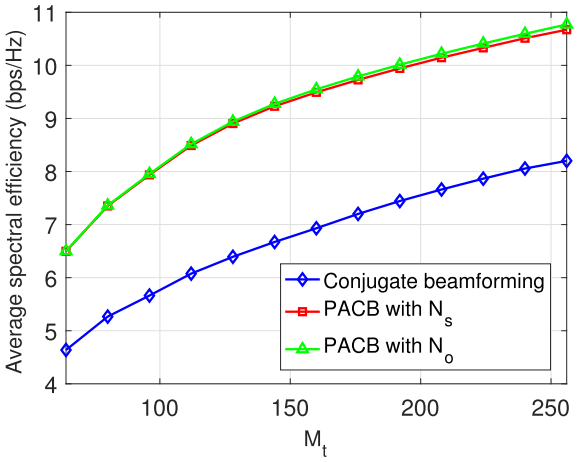

FIGURE 5. Case two (two-user): comparison of average SE for different numbers of transmit antennas.

B. CASE TWO (TWO-USER)

In this case, we set SNR $=$ 0 dB and vary the number of transmit antennas $M_{\rm t}$. The rest of the system's parameters are as in *Case One*. Fig. 5 compares the downlink SEs achieved by the conventional CB and the PACB as the functions of the number of transmit antennas. Observe that an average of 2 bps/Hz performance gain is attained by the PACB over the conventional CB. This further validates the theoretical analysis for $C_{\rm s} \gg C_{\rm f}$ presented in Section III-C. The results of Fig. 5 also confirm that $C_{\rm s} \approx C_{\rm o}$.

C. CASE THREE (TWO-USER)

We then set SNR $=$ 0 dB and vary δ from 2° to 10°. The rest of the system's parameters are as in *Case One*. Observe from Fig. 6 that the performance of the conventional CB degrades quickly as δ decreases. This agrees with the analysis of Section II that the CB with all the $M_{\rm t}$ antennas activated is unable to handle the scenario of close users effectively. When δ decreases, ε becomes smaller. As shown in Section II, as $\varepsilon \to 0$, the IUI suffered by the CB with all the $M_{\rm t}$ antennas activated approaches its maximum value. By contrast, observed from Fig. 6 that the performance gain of the proposed PACB scheme over the conventional CB increases as δ decreases. According to (24), the upper-bound of $q(N_{\rm s})$ approaches 0 as $\varepsilon \to 0$. Therefore, compared to the fixed residual $q(M_{\rm t})$, the IUI reduction capability of the PACB becomes more significant with smaller ε, which leads to larger performance gain over the conventional CB.

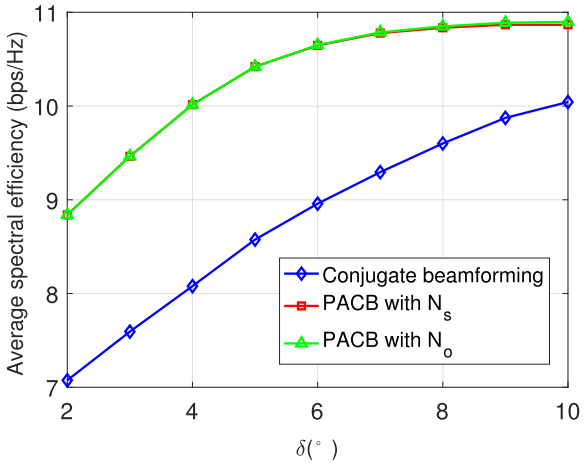

FIGURE 6. Case three (two-user): comparison of average SE for various differences between the two AoDs.

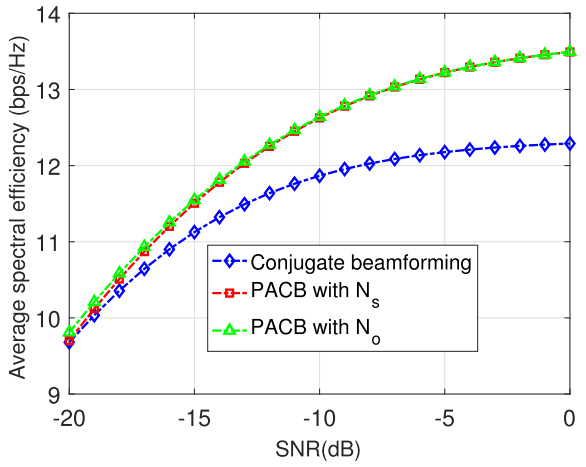

FIGURE 7. Case four (four-user): comparison of average SE for different SNRs.

D. CASE FOUR (FOUR-USER)

Again the BS is equipped with $M_{\mathrm{t}} = 128$ transmit antennas, while each of the four users employs $M_{\mathrm{r}} = 16$ receive antennas. The four users' AoDs, φ_i for $1 \leq i \leq 4$, are related by $\varphi_i = \varphi_1 + \delta_i$, $i = 2, 3, 4$, where all the three δ_i are uniformly distributed in $(0,\ 5^\circ)$. Fig. 7 compares the downlink SEs achieved by the conventional CB and the PACB as the functions of SNR. As in *Case One* with two users, it can be seen that the PACB significantly outperforms the conventional CB.

E. CASE FIVE (TWO-USER)

Besides the above results obtained under pure LoS channels, additional comparisons of average spectral efficiency assuming different numbers of NLoS sub-paths are presented in Fig. 8, in which $P = 3, 6$ and $E\{|\alpha_0|\}/E\{|\alpha_p|\} = 10$dB are adopted. Obviously, the average spectral efficiency degenerates with more numbers of NLoS sub-paths. However, the PACB still outperforms the conventional CB considerably with different numbers of NLoS sub-paths.

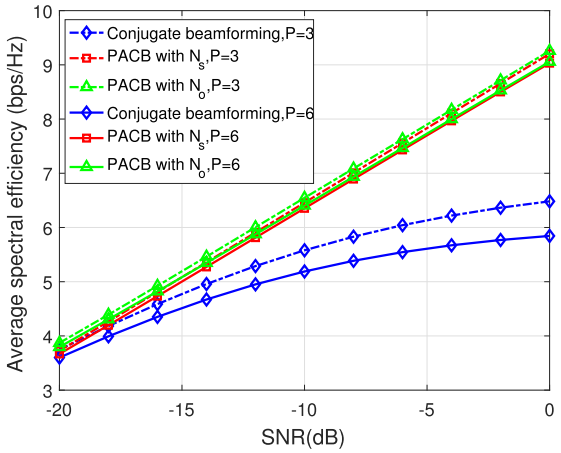

FIGURE 8. Case five (two-user): comparison of average SE for different numbers of NLoS sub-paths.

V. CONCLUSIONS

The PACB scheme has been proposed for LoS-dominant massive communication systems, especially with adjacent users. By exploiting the structure of LoS channel, the proposed PACB activates only a fraction of the transmit antennas for beamforming, and the optimal number of activated antennas can be determined by maximizing the system's downlink capacity using an exhaustive search, which has the complexity that is linear to the number of total available antennas. Alternatively, we have derived an even lower complexity searching algorithm to determine the number of activated antennas by maximizing the system's SIR only. Both theoretical analysis and simulation investigation have shown that the performance achieved by the PACB with this low-complexity search algorithm is indistinguishable from that achieved by the optimal PACB solution. More importantly, both theoretical analysis and simulation results have demonstrated that the PACB scheme offers significantly higher downlink spectral efficiency compared to the conventional conjugate beamforming counterpart.

REFERENCES

[1] F. Rusek *et al.*, "Scaling up MIMO: Opportunities and challenges with very large arrays," *IEEE Signal Process. Mag.*, vol. 30, no. 1, pp. 40–60, Jan. 2013.

[2] H. Q. Ngo, E. G. Larsson, and T. L. Marzetta, "Energy and spectral efficiency of very large multiuser MIMO systems," *IEEE Trans. Commun.*, vol. 61, no. 4, pp. 1436–1449, Apr. 2013.

[3] H. Yang and T. L. Marzetta, "Performance of conjugate and zero-forcing beamforming in large-scale antenna systems," *IEEE J. Sel. Areas Commun.*, vol. 31, no. 2, pp. 172–179, Feb. 2013.

[4] E. G. Larsson, O. Edfors, F. Tufvesson, and T. L. Marzetta, "Massive MIMO for next generation wireless systems," *IEEE Commun. Mag.*, vol. 52, no. 2, pp. 186–195, Feb. 2014.

[5] O. N. Alrabadi, E. Tsakalaki, H. Huang, and G. F. Pedersen, "Beamforming via large and dense antenna arrays above a clutter," *IEEE J. Sel. Areas Commun.*, vol. 31, no. 2, pp. 314–325, Feb. 2013.

[6] J. Choi, "Multiuser precoding with limited cooperation for large-scale MIMO multicell downlink," *IEEE Trans. Wireless Commun.*, vol. 14, no. 3, pp. 1295–1308, Mar. 2015.

[7] S. K. Mohammed and E. G. Larsson, "Constant-envelope multi-user precoding for frequency-selective massive mimo systems," *IEEE Wireless Commun. Lett.*, vol. 2, no. 5, pp. 547–550, Oct. 2013.
[8] J. Zhang, S. Chen, R. G. Maunder, R. Zhang, and L. Hanzo, "Adaptive coding and modulation for large-scale antenna array-based aeronautical communications in the presence of co-channel interference," *IEEE Trans. Wireless Commun.*, vol. 17, no. 2, pp. 1343–1357, Feb. 2018.
[9] Y. Zeng, R. Zhang, and T. J. Lim, "Wireless communications with unmanned aerial vehicles: Opportunities and challenges," *IEEE Commun. Mag.*, vol. 54, no. 5, pp. 36–42, May 2016.
[10] T. J. Willink, C. C. Squires, G. W. K. Colman, and M. T. Muccio, "Measurement and characterization of low-altitude air-to-ground MIMO channels," *IEEE Trans. Veh. Technol.*, vol. 65, no. 4, pp. 2637–2648, Apr. 2015.
[11] W. Roh *et al.*, "Millimeter-wave beamforming as an enabling technology for 5G cellular communications: Theoretical feasibility and prototype results," *IEEE Commun. Mag.*, vol. 52, no. 2, pp. 106–113, Feb. 2014.
[12] A. L. Swindlehurst, E. Ayanoglu, P. Heydari, and F. Capolino, "Millimeter-wave massive MIMO: The next wireless revolution?" *IEEE Commun. Mag.*, vol. 52, no. 9, pp. 56–62, Sep. 2014.
[13] K. Guan *et al.*, "On millimeter wave and THz mobile radio channel for smart rail mobility," *IEEE Trans. Veh. Technol.*, vol. 66, no. 7, pp. 5658–5674, Jul. 2017.
[14] O. El Ayach, S. Rajagopal, S. Abu-Surra, Z. Pi, and R. W. Heath, Jr., "Spatially sparse precoding in millimeter wave MIMO systems," *IEEE Trans. Wireless Commun.*, vol. 13, no. 3, pp. 1499–1513, Mar. 2014.
[15] J.-C. Chen, "Efficient codebook-based beamforming algorithm for millimeter-wave massive MIMO systems," *IEEE Trans. Veh. Technol.*, vol. 66, no. 9, pp. 7809–7817, Sep. 2017.
[16] L. Liang, W. Xu, and X. Dong, "Low-complexity hybrid precoding in massive multiuser MIMO systems," *IEEE Wireless Commun. Lett.*, vol. 3, no. 6, pp. 653–656, Dec. 2014.
[17] *MIMO Transmission Schemes for NR*, document 17 R1-1609905, InterDigital Communications, 3GPP TSG-RAN WG1 #86bis, Lisbon, Portugal, Oct. 2016.
[18] M. Agiwal, A. Roy, and N. Saxena, "Next generation 5G wireless networks: A comprehensive survey," *IEEE Commun. Surveys Tut.*, vol. 18, no. 3, pp. 1617–1655, 3rd Quart., 2016.
[19] *On MU MIMO Nonlinear Precoding in NR*, document 19 R1-1701087, Nokia, Alcatel-Lucent Shanghai Bell, 3GPP TSG-RAN WG1 #Ad-Hoc, Spokane, WA, USA, Jan. 2017.
[20] P. Zhang, S. Chen, and L. Hanzo, "Two-tier channel estimation aided near-capacity MIMO transceivers relying on norm-based joint transmit and receive antenna selection," *IEEE Trans. Wireless Commun.*, vol. 14, no. 1, pp. 122–137, Jan. 2015.
[21] N. N. Alotaibi and K. A. Hamdi, "Switched phased-array transmission architecture for secure millimeter-wave wireless communication," *IEEE Trans. Commun.*, vol. 64, no. 3, pp. 1303–1312, Mar. 2016.
[22] N. Valliappan, A. Lozano, and R. W. Heath, Jr., "Antenna subset modulation for secure millimeter-wave wireless communication," *IEEE Trans. Commun.*, vol. 61, no. 8, pp. 3231–3245, Aug. 2013.
[23] T. S. Rappaport, E. Ben-Dor, J. N. Murdock, and Y. Qiao, "38 GHz and 60 GHz angle-dependent propagation for cellular & peer-to-peer wireless communications," in *Proc. IEEE Int. Conf. Commun. (ICC)*, Jun. 2012, pp. 4568–4573.
[24] G. Zhu, K. Huang, V. K. N. Lau, B. Xia, X. Li, and S. Zhang, "Hybrid beamforming via the Kronecker decomposition for the millimeter-wave massive MIMO systems," *IEEE J. Sel. Areas Commun.*, vol. 35, no. 9, pp. 2097–2114, Sep. 2017.

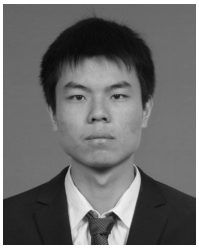

WENDONG LIU received the B.S. degree (Hons.) from Tsinghua University, Beijing, China, in 2015, where he is currently pursuing the Ph.D. degree with the Department of Electronic Engineering. His research interests include massive MIMO, full-dimension MIMO, and millimeter-wave communications.

ZHAOCHENG WANG (M'09–SM'11) received the B.S., M.S., and Ph.D. degrees from Tsinghua University, Beijing, China, in 1991, 1993, and 1996, respectively. From 1996 to 1997, he was a Post-Doctoral Fellow with Nanyang Technological University, Singapore. From 1997 to 1999, he was with OKI Techno Centre Pte. Ltd., Singapore, where he was first a Research Engineer and later became a Senior Engineer. From 1999 to 2009, he was with Sony Deutschland GmbH, where he was first a Senior Engineer and later became a Principal Engineer. He is currently a Professor of electronic engineering with Tsinghua University and serves as the Director of the Broadband Communication Key Laboratory, Tsinghua National Laboratory for Information Science and Technology. He has authored or co-authored over 120 journal papers. He holds 34 granted U.S./EU patents. He has co-authored two books, one of which, *Millimeter Wave Communication Systems*, was selected by IEEE Series on Digital and Mobile Communication (Wiley-IEEE Press). His research interests include wireless communications, visible light communications, millimeter-wave communications, and digital broadcasting. He is a fellow of the Institution of Engineering and Technology. He served as the Associate Editor of the IEEE TRANSACTIONS ON WIRELESS COMMUNICATIONS from 2011 to 2015 and IEEE COMMUNICATIONS LETTERS from 2013 to 2016, and has also served as the technical program committee co-chair of various international conferences.

JIANFEI CAO received the B.S. degree from Hunan University, and the Ph.D. degree from Beijing Jiaotong University, China, in 2006 and 2012, respectively. From 2009 to 2010, he was a Visiting Ph.D. Student with the University of Southampton, U.K. From 2012 to 2014, he was an Associate Researcher with the NEC Laboratory, China. From 2014 to 2016, he was a Senior Engineer with the Samsung Research Laboratory, China. Since 2016, he has been a Vice-Manager with the SONY China Research Laboratory. His research interests include FD-MIMO in LTE and massive MIMO in 5G NR.

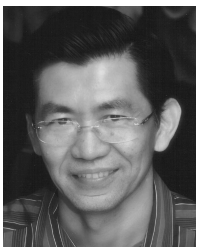

SHENG CHEN (M'90–SM'97–F'08) received the B.Eng. degree in control engineering from the East China Petroleum Institute, Dongying, China, in 1982, the Ph.D. degree in control engineering from City University, London, in 1986, and the D.Sc. degree from the University of Southampton, Southampton, U.K., in 2005.

From 1986 to 1999, he held research and academic appointments at the Universities of Sheffield, Edinburgh, and Portsmouth, all in U.K. Since 1999, he has been with the School of Electronics and Computer Science, University of Southampton, U.K., where he is currently a Professor in intelligent systems and signal processing. His research interests include adaptive signal processing, wireless communications, modeling and identification of nonlinear systems, neural network and machine learning, intelligent control system design, evolutionary computation methods, and optimization. He has published over 600 research papers. He is a fellow of the United Kingdom Royal Academy of Engineering, a fellow of IET, a Distinguished Adjunct Professor at King Abdulaziz University, Jeddah, Saudi Arabia, and an ISI highly cited researcher in engineering in 2004. He has 11400 Web of Science citations and over 24 000 Google Scholar citations.

LAJOS HANZO (F'04) received the D.Sc. degree in electronics in 1976 and the Ph.D. degree in 1983. During his 40-year career in telecommunications, he has held various research and academic posts in Hungary, Germany, and U.K. Since 1986, he has been with the School of Electronics and Computer Science, University of Southampton, U.K., where he holds the Chair in telecommunications. In 2016, he was admitted to the Hungarian Academy of Science. He has successfully supervised 111 Ph.D. students, co-authored 18 John Wiley/IEEE Press books on mobile radio communications totaling in excess of 10 000 pages, published 1780 research contributions at IEEE Xplore, acted both as the TPC and general chair of IEEE conferences, presented keynote lectures, and has been awarded. a number of distinctions. He is currently directing a 60-strong academic research team, working on a range of research projects in the field of wireless multimedia communications sponsored by industry, the Engineering and Physical Sciences Research Council, U.K., the European Research Council's Advanced Fellow Grant, and the Royal Society's Wolfson Research Merit Award. He is an enthusiastic supporter of industrial and academic liaison, and he offers a range of industrial courses. He is a fellow of the Royal Academy of Engineering, the Institution of Engineering and Technology, and the European Association for Signal Processing. In 2009, he was a recipient of the honorary doctorate by the Technical University of Budapest and in 2015 by The University of Edinburgh. He is also the Governor of the IEEE ComSoc and VTS. From 2008 to 2012, he was the Editor-in-Chief of the IEEE Press and a Chaired Professor at Tsinghua University, Beijing.